HHS Public Access

Author manuscript

Nature. Author manuscript; available in PMC 2014 April 03.

Published in final edited form as:

Nature. 2013 October 3; 502(7469): 105–109. doi:10.1038/nature12501.

Podoplanin maintains high endothelial venule integrity by interacting with platelet CLEC-2

Brett H. Herzog[1,2,*], **Jianxin Fu**[1,3,4,*], **Stephen J. Wilson**[5], **Paul R. Hess**[6], **Aslihan Sen**[6], **J. Michael McDaniel**[1], **Yanfang Pan**[1,2], **Minjia Sheng**[1], **Tadayuki Yago**[1], **Robert Silasi-Mansat**[1], **Samuel McGee**[1], **Frauke May**[7], **Bernhard Nieswandt**[7], **Andrew J. Morris**[8], **Florea Lupu**[1], **Shaun R. Coughlin**[5], **Rodger P. McEver**[1,2], **Hong Chen**[1,2], **Mark L. Kahn**[6], and **Lijun Xia**[1,2,3,4]

[1]Cardiovascular Biology Research Program, Oklahoma Medical Research Foundation, Oklahoma City, Oklahoma 73104, USA

[2]Department of Biochemistry and Molecular Biology, University of Oklahoma Health Sciences Center, Oklahoma City, Oklahoma 73104, USA

[3]Jiangsu Institute of Hematology, The First Affiliated Hospital of Soochow University, Suzhou, Jiangsu 215006, China

[4]Key Laboratory of Thrombosis and Hemostasis of Ministry of Health, The First Affiliated Hospital of Soochow University, Suzhou, Jiangsu 215006, China

[5]Cardiovascular Research Institute, University of California, San Francisco, California 94158, USA

[6]Department of Medicine and Cardiovascular Institute, University of Pennsylvania, Philadelphia, Pennsylvania 19104, USA

[7]University Hospital Wurzburg and Rudolf Virchow Center, DFG-Research Center for Experimental Biomedicine, Wurzburg, Germany

[8]Division of Cardiovascular medicine, University of Kentucky and Veterans Affairs Medical Center, Lexington, Kentucky 40502, USA

Abstract

Circulating lymphocytes continuously enter lymph nodes (LNs) for immune surveillance through specialised blood vessels named high endothelial venules (HEVs)[1–5], a process that increases dramatically during immune responses. How HEVs permit lymphocyte transmigration while

Correspondence: Lijun Xia, Cardiovascular Biology Research Program, Oklahoma Medical Research Foundation, 825 N.E. 13th Street, Oklahoma City, OK 73104; Tel: (405) 271-7892; FAX: (405) 271-3137; Lijun-Xia@omrf.org.

*These authors contributed equally to this study.

Author contributions

B.H.H. and J.F. designed and performed experiments, analyzed results, and drafted the manuscript. J.M.M., Y.P., M.S., T.Y., R.S.-M., F.L., A.J.M. and S.M. performed experiments. S.J.W., S. R. C., F.M., B.N., A.S., and P.R.H. supplied key reagents and mice. R.P.M., H.C., and M.L.K. helped analyse results and commented on the manuscript. L.X. designed and supervised research and wrote the manuscript.

The authors declare no competing financial interests.

maintaining vascular integrity is unknown. Here, we report a role for the transmembrane O-glycoprotein podoplanin (PDPN, also known as gp38 and T1α)[6–8] in maintaining HEV barrier function. Mice with postnatal deletion of PDPN lost HEV integrity and exhibited spontaneous bleeding in mucosal LNs, and bleeding in the draining peripheral LN after immunisation. Blocking lymphocyte homing rescued bleeding, indicating that PDPN is required to protect the barrier function of HEVs during lymphocyte trafficking. Further analyses demonstrated that PDPN expressed on fibroblastic reticular cells (FRCs)[7], which surround HEVs, functions as an activating ligand for platelet C-type lectin-like receptor 2 (CLEC-2)[9,10]. Mice lacking FRC PDPN or platelet CLEC-2 exhibited significantly reduced levels of VE-cadherin (VE-cad), which is essential for overall vascular integrity[11,12], on HEVs. Infusion of wild-type (WT) platelets restored HEV integrity in CLEC-2-deficient mice. Activation of CLEC-2 induced release of sphingosine-1-phosphate (S1P)[13,14] from platelets, which promoted expression of VE-cad on HEVs ex vivo. Furthermore, draining peripheral LNs of immunised mice lacking S1P had impaired HEV integrity similar to PDPN- and CLEC-2-deficient mice. These data demonstrate that local S1P release after PDPN-CLEC-2-mediated platelet activation is critical for HEV integrity during immune responses.

LNs are essential sites for immune responses. They are organised into lobules, which are surrounded by lymphatic sinuses that deliver antigens from afferent lymphatic vessels to LNs for identification by naïve lymphocytes that continually home through HEVs (Supplementary Fig. 1). Lymphocyte trafficking is particularly prominent in mucosal LNs, as the majority of foreign antigens enter the body through mucosal epithelium, and in draining peripheral LNs during immune responses[1,15]. How HEVs accommodate a high rate of lymphocyte trafficking while maintaining their integrity remains unknown.

Platelets support vascular integrity in inflamed tissues by still undefined mechanisms[16]. Whether and if so, how platelets protect HEV integrity in the LN is unexplored. PDPN, a ligand for the platelet activating receptor CLEC-2, is highly expressed in LNs. We developed mice with tamoxifen (TM)-inducible global deletion of PDPN (*Pdpn$^{f/f}$;CagCre*, Supplementary Fig. 2a–d), and focused first on the mucosal LNs of mice around the weaning-age because development of adaptive immunity occurs early and primarily through mucosal LNs[17]. TM administration from postnatal day 1 (P1) through P5 resulted in ~90% reduction of PDPN at P15 and complete loss at 1 month in both mucosal and peripheral LNs (Supplementary Figs. 2e, 3a–b, d). Beginning at P15 and progressively worsening, *Pdpn$^{f/f}$;CagCre* pups exhibited massive bleeding primarily in mucosal LNs including mesenteric LNs (MLNs) and cervical LNs (CLNs) (Supplementary Fig. 3e–f) but rarely in peripheral (inguinal and popliteal) LNs (Fig. 1a, Supplementary Fig. 3a–f). Histology and confocal imaging of MLNs revealed large numbers of extravasated red blood cells (RBCs) around HEVs but not non-HEV vessels of *Pdpn$^{f/f}$;CagCre* mice (Fig. 1b–d). PDPN deletion starting at 3-4 weeks of age resulted in a similar mucosal LN bleeding phenotype, suggesting that PDPN is also important for LN vascular integrity in adults (Supplementary Fig. 3c–d).

In LNs, PDPN is expressed by endothelial cells of lymphatic vessels but not by blood vessels including HEVs (Supplemental Fig. 4a). However, PDPN is also highly expressed

on FRCs, which surround HEVs and express ER-TR7, αSMA, and PDGFRβ [7,18](Supplementary Fig. 4b–d). To address whether PDPN on FRCs is essential for LN vascular integrity, we generated *Pdpn$^{f/f}$;PdgfrbCre* mice, which lack PDPN in FRCs but otherwise exhibit normal FRC organization (Supplementary Fig. 5b, e). Similar to *Pdpn$^{f/f}$;CagCre* mice, *Pdpn$^{f/f}$;PdgfrbCre* mice developed bleeding in mucosal LNs (Fig. 1e). *Pdpn$^{f/f}$;PdgfrbCre* mice also had reduced levels of PDPN on lymphatic endothelial cells (LECs) in LNs (Supplementary Fig. 5b–d). To rule out the contribution of endothelial PDPN to LN bleeding, we developed *Pdpn$^{f/f}$;Tie2Cre* mice, which lack PDPN specifically in LECs but not in FRCs (Supplementary Fig. 6a–d). Consistent with the previously described role of PDPN in the separation of blood and lymphatic vessels during embryonic development[8], *Pdpn$^{f/f}$;Tie2Cre* mice exhibited blood-lymphatic vessel mixing phenotype (Supplementary Fig. 6e, data not shown). However, *Pdpn$^{f/f}$;Tie2Cre* mice did not exhibit bleeding around HEVs in the LN (Supplementary Fig. 6e–f). These results indicate that PDPN on FRCs rather than LECs prevents bleeding in LNs.

CLEC-2 is the only known receptor for PDPN[9,10,19]. To determine its importance for LN vascular integrity, we depleted CLEC-2 in WT neonates using a CLEC-2-specific monoclonal antibody (mAb), INU1[19]. Administration of INU1 resulted in bleeding in mucosal LNs at P15 similar to *Pdpn$^{f/f}$;CagCre* mice (Fig. 1f, Supplementary Fig. 7a). To determine the role of CLEC-2 in adult LNs, we made *Clec-2$^{-/-}$* bone marrow chimaeras (*Clec-2$^{-/-}$* BM chimaera, Supplementary Fig. 7b–c), which, consistent with deleting PDPN in adult mice, developed bleeding in mucosal LNs (Supplementary Fig. 7d). CLEC-2 is primarily expressed on platelets[10,19]; however, it is also expressed on myeloid and dendritic cells. To verify whether CLEC-2 on platelets is required to protect LN vascular integrity, we developed mice lacking CLEC-2 specifically on platelets (*Clec-2$^{f/f}$;Pf4Cre*, Supplemental Fig. 8a–c). *Clec-2$^{f/f}$;Pf4Cre* mice developed spontaneous bleeding in mucosal LNs reminiscent of PDPN-deficient mice (Fig. 1g, Supplemental Fig. 8d). Collectively, these results indicate that FRC PDPN and platelet CLEC-2 are required to protect LN vascular integrity.

To explore where platelet CLEC-2 interacts with PDPN in the LN, we stained cryosections of LNs and found frequent associations of platelets with PDPN^{+} FRCs at the abluminal sides of HEVs of WT but not PDPN-deficient mice (Fig. 2a, Supplemental Fig. 9). Furthermore, intravenously transfused fluorescently labelled CLEC-2-expressing WT platelets were detected on the abluminal sides of HEVs in close association with PDPN^{+} FRCs of *Clec-2$^{-/-}$* BM chimaeras (Fig. 2b), supporting that platelets interact with FRCs around HEVs in a PDPN-CLEC-2-dependent manner.

Mucosal LNs but not peripheral LNs of PDPN- or CLEC-2-deficient mice exhibit spontaneous bleeding, suggesting phenotypic differences between these two types of LNs. We found that mucosal LNs were significantly more permeable to Evans blue dye than peripheral LNs in the steady-state (Fig. 2c). We noted that mucosal but not peripheral HEVs express MAdCAM-1 (Supplementary Fig. 10a–b). However, after an immune challenge (ovalbumin/complete Freund's adjuvant, OVA/CFA), HEVs in peripheral LNs of WT mice had increased MAdCAM-1 expression and permeability, resembling mucosal HEVs (Supplementary Fig. 10b, data not shown). Importantly, *Pdpn$^{f/f}$;CagCre* or *Clec-2$^{f/f}$;Pf4Cre*

but not WT mice developed bleeding in draining peripheral LNs after OVA/CFA challenge (Fig. 2d). These results suggest a crucial role for PDPN-CLEC-2 interactions in maintaining vascular integrity of steady-state mucosal and immunised peripheral LNs, which share a similar "*reactive*" functional and molecular phenotype and are specifically vulnerable to bleeding. Consistent with this, bleeding was observed in mucosal LNs of 3-week-old *Pdpn*$^{f/f}$*;PdgfrbCre* mice, but not *Pdpn*$^{f/f}$*;PdgfrbCre* mice bred into a *Rag1*$^{-/-}$ background that lack lymphocytes (Fig. 2e). In addition, depleting CLEC-2 with INU1 resulted in mucosal LN bleeding in 2-week-old WT but not *Rag1*$^{-/-}$ mice, highlighting the importance of lymphocytes in promoting mucosal LN bleeding (Supplementary Fig. 11a). We next administered a mAb to L-selectin (Mel-14) that blocks lymphocyte trafficking through HEVs (Supplementary Fig. 11b)[20]. Mel-14 significantly reduced the bleeding observed in the draining peripheral LN of immunised *Pdpn*$^{f/f}$*;CagCre* mice compared with an isotype control (Fig. 2f, Supplementary Fig. 11c). A previous study shows that activated platelets facilitate lymphocyte adhesion to HEVs[21]. However, whether platelets transmigrate with or following lymphocytes to the abluminal space of HEVs to fulfill additional function is unknown. We found that draining peripheral LNs from immunised WT mice had a significant increase in the number of platelets at the abluminal sides of HEVs, which was abolished after Mel-14 treatment, demonstrating that platelets migrate across HEVs in a lymphocyte transmigration-dependent manner to interact with FRCs (Supplemental Fig. 11d). These data support that interactions between platelets and FRCs are critical for preventing bleeding in "*reactive*" LNs during immune responses when lymphocyte trafficking is increased.

To determine whether impaired HEV barrier function is responsible for the observed LN bleeding when PDPN is absent, we intravenously injected FITC-dextran immediately prior to euthanasia. FITC-dextran was contained within HEVs of WT MLNs. However, FITC-dextran leaked from HEVs, but not from non-HEV blood vessels in LNs and other organs, of *Pdpn*$^{f/f}$*;CagCre* mice (Fig. 3a, Supplementary Fig. 12a, and data not shown). Furthermore, intravenously injected, fluorescently labelled RBCs were detected outside of HEVs in *Pdpn*$^{f/f}$*;CagCre* but not in WT mice (Fig. 3b). Ultrastructural analyses indicated that abnormal gaps between endothelial cell membranes were specific to HEVs of *Pdpn*$^{f/f}$*;CagCre* mice, and RBCs were frequently observed between or outside of high endothelial cells in *Pdpn*$^{f/f}$*;CagCre* mice (Fig. 3c, Supplemental Fig. 12b). Together, these data indicate that, in the absence of PDPN, impaired vascular barrier function and defective junctions are restricted to HEVs.

VE-cadherin (VE-cad) is an integral component of endothelial adherens junctions and barrier function[22]. We found that levels of VE-cad were reduced in HEVs of *Pdpn*$^{f/f}$*;CagCre* MLNs starting at P8, prior to the onset of bleeding (Fig. 3d, Supplemental Fig. 12c–d), consistent with the idea that loss of HEV junctional integrity contributes to the onset of bleeding. Furthermore, following the loss of PDPN, β-catenin, another component of endothelial adherens junctions[22], was decreased (Supplemental Fig. 12e) and expression of N-cadherin, which is essential for endothelial-stromal cell junctions[22], was reduced around HEVs (Supplemental Fig. 12f). Further analyses indicate that VE-cad was expressed at higher levels in peripheral HEVs than in mucosal HEVs of WT mice (Supplemental Fig.

13a). ZO-1[22], another junction molecule, was detected on peripheral but not mucosal HEVs. However, HEVs in draining peripheral LNs of immunised WT mice exhibited reduced VE-cad and ZO-1 expression, resembling MLNs of WT mice (Supplemental Fig. 13a, b). Consistent with the bleeding in draining peripheral LNs (Fig. 2d) of immunised PDPN- or CLEC-2-deficient mice, these LNs exhibited a further reduction of VE-cad on their HEVs (Supplemental Fig. 13a), which was normalised by blocking lymphocyte trafficking with Mel-14 (Supplemental Fig. 13c). Furthermore, blocking VE-cad increased permeability in draining peripheral LNs of immunised WT mice (Supplemental Fig. 14). These results support the idea that interactions of PDPN and CLEC-2 preserve HEV barrier function primarily by promoting VE-cad expression on HEVs.

HEVs of *Clec-2*$^{-/-}$ BM chimaeras exhibited increased permeability to intravenously injected FITC-dextran (Fig. 3e). To test whether this phenotype could be rescued by WT platelets, *Clec-2*$^{-/-}$BM chimaeras were transfused daily with WT platelets for 4 days prior to euthanasia. HEVs of *Clec-2*$^{-/-}$ BM chimaeras that received WT platelets exhibited significantly decreased permeability to FITC-dextran compared to controls (Fig. 3e). Significantly, WT and *Clec-2*$^{-/-}$ BM chimaeras transfused with WT platelets expressed comparable levels of VE-cad on HEVs (Fig. 3f, Supplemental Fig. 15). Together, these results demonstrate that PDPN and platelet CLEC-2 are essential for preserving adherens junctions of HEVs.

Platelet aggregation is essential for hemostasis[16,23]. However, blocking aggregation with a mAb to integrin αIIbβ3 did not increase permeability in draining peripheral LNs of immunised WT mice (Supplemental Fig. 14). This suggests that a platelet function mediated by PDPN-CLEC-2 apart from aggregation is required for HEV integrity. Sphingosine-1-phosphate (S1P)[13,14], a bioactive lipid, is a strong candidate for mediating this platelet function as it is known to regulate vascular integrity through interactions with its G protein-coupled receptors on endothelial cells[13].

Although platelets generate and store S1P[24], whether PDPN-CLEC-2-mediated platelet activation causes S1P release is unknown. To test this, we stimulated WT and *Clec-2*$^{-/-}$ platelets with the mAb INU1, which activates CLEC-2 signaling in vitro[19], and observed a CLEC-2-dependent S1P release from platelets (Fig. 4a). Furthermore, PDPN^{+} but not PDPN^{-} melanoma cells induced the release of S1P from WT but not *Clec-2*$^{-/-}$ platelets (Supplemental Fig. 16a–b), indicating that interactions between PDPN and CLEC-2 induce S1P release from platelets. Next, we found that MLN slices cultured ex vivo with fetal bovine serum (FBS), but not lipid-depleted FBS, retained VE-cad expression on their HEVs (Fig. 4b, Supplemental Fig. 16c), supporting the idea that a lipid, such as S1P, maintains HEV adherens junctions. The addition of WT but not *Clec-2*$^{-/-}$ platelets rescued VE-cad levels on HEVs of MLN slices cultured in lipid-depleted FBS-containing media. WT platelets were unable to restore HEV VE-cad expression on MLN slices from PDPN-deficient mice (Fig. 4b, Supplemental Fig. 16c), demonstrating that FRC PDPN and platelet CLEC-2 are required for normal VE-cad expression on HEVs. The increase of VE-cad on HEVs in the presence of WT platelets is due, at least in part, to the activation of the S1P receptor 1 (S1PR1), because the S1PR1 antagonist, W146[14], blocked the WT platelet-induced VE-cad expression on HEVs (Fig. 4b, Supplemental Fig. 16c). Furthermore,

platelets from WT, but not S1P-deficient (S1Pless) mice[13], rescued VE-cad expression on HEVs of MLNs (Fig. 4b, Supplemental Fig. 16c), supporting the importance of platelet S1P. S1Pless mice did not develop spontaneous mucosal LN bleeding, likely due to reduced lymphocyte transmigration through HEVs because of lower circulating lymphocytes[25] (Supplemental Fig. 17a). However, after OVA/CFA challenge of the hindlimb, the draining peripheral LNs of S1Pless mice exhibited bleeding, increased permeability to FITC-dextran, and decreased VE-cad expression on HEVs, resembling mice lacking PDPN or CLEC-2 (Fig 4c–d, Supplemental Fig. 17b–d). A daily transfusion (for four consecutive days) of WT but not *Clec-2*$^{-/-}$ platelets resulted in higher levels of VE-cad on HEVs and reduced vascular leak of injected FITC-dextran from HEVs of draining peripheral LNs of immunised S1Pless mice (Fig. 4d, Supplemental Fig. 18). Taken together, these data indicate that PDPN-CLEC-2-dependent local release of S1P from platelets plays a critical role in maintaining HEV integrity during immune responses.

Unlike other venules, HEVs are not circumscribed by typical pericytes and collagen-containing matrix that would activate platelets. Instead, they are surrounded by a perivenular sleeve of FRCs that sequester collagen fibers[26,27]. Our findings reveal an important new role for FRC PDPN (Fig. 4e), which is well positioned to interact with CLEC-2 on extravasated platelets. S1P in the blood is known to regulate vascular integrity[13]. Our data demonstrate that PDPN-CLEC-2-dependent platelet activation causes release of S1P in the perivenular space that preserves VE-cad expression on HEVs (Fig. 4e). Thus, cross-talk between FRCs, platelets, and HEVs is essential to maintain HEV integrity in situations of increased lymphocyte trafficking such as chronic inflammation. Recently, components of CLEC-2 signaling pathway have been implicated in preventing inflammation-induced hemorrhage in the skin and lung[28]. Therefore, PDPN-CLEC-2-mediated local S1P release from platelets may protect vascular integrity in other inflamed tissues.

Full Methods

Mice

To generate mice with loxP-flanked *Pdpn* alleles (*Pdpn*$^{f/f}$), a targeting vector was constructed in which exon 2, the major coding exon of *Pdpn* gene, was flanked by loxP sites (*Pdpn*$^{f/f}$), and the neomycin resistance selection cassette (Neo) was flanked by Frt sites (Supplementary Fig. 2a). The Not I-linearized construct was electroporated into C57BL/6-derived embryonic stem (ES) cells, and correctly targeted clones were identified by Southern blots. The Frt-flanked Neo was removed by transient expression of Flp recombinase in the positive ES clones to avoid potential undesirable effects of the Neo cassette. ES cells with normal karyotype bearing a floxed *Pdpn* allele were microinjected into B6/Tyr blastocytes, which were subsequently implanted into pseudopregnant foster mothers. Male chimaeras were bred with C57BL/6J females for germline transmission. Heterozygous mice were then crossed to generate *Pdpn*$^{f/f}$ mice (Supplemental Fig. 2a-b).

To generate mice with inducible deletion of PDPN (*Pdpn*$^{f/f}$*;CagCre*), *Pdpn*$^{f/f}$ mice were crossed with the CAG-Cre-ER^{T2} Tg mice (B6.Cg-Tg(CAG-cre/Esr1*)5Amc/J, Jackson Laboratories)[29]. To induce postnatal deletion of PDPN, tamoxifen (TM, MP Biomedical) was dissolved in ethanol/sunflower oil (1:9) and administered orally (p.o.) (20 μg per day) to

pups from postnatal day (P) 1-5. Adult deletion was accomplished by administering TM p.o. (1 mg per day) for 5 consecutive days beginning at P21, then once a week thereafter. Wild-type littermates (WT, *Pdpn*$^{f/w}$*;CagCre* or *Pdpn*$^{f/f}$) treated with the same regimen were used as controls. Mice deficient for PDPN in pericytes/fibroblasts including FRCs (*Pdpn*$^{f/f}$*;PdgfrbCre*) or in endothelial cells (*Pdpn*$^{f/f}$*;Tie2Cre)* were generated by crossing *Pdpn*$^{f/f}$ mice with *PdgfrbCre* Tg mice [Tg(Pdgfrb-cre)9Rha][30] or *Tie2Cre* Tg mice [Tg(Tek-cre)1Ywa][31], respectively.

CLEC-2 conditional mice were generated in which exons 3 and 4 of the *Clec-2* allele are flanked by loxP sites (*Clec-2*$^{f/f}$). Deletion of exons 3 and 4 induces a premature stop codon that blocks the expression of CLEC-2's extracellular domain (Supplementary Fig. 8a). ES clones with correct homologous recombination were microinjected into B6 blastocytes, which were subsequently implanted into pseudopregnant foster mothers. Male chimaeras were bred with ACTB-FLP1 females (B6.Cg-Tg(ACTFLPe)9205Dym/J, Jackson Laboratory) for germline transmission and removal of the Neo cassette. Heterozygous mice were then crossed to generate *Clec-2*$^{f/f}$ mice. *Clec-2*$^{f/f}$ mice were crossed with *Pf4Cre* Tg mice (C57BL/6-Tg(Pf4-cre)Q3Rsko/J, Jackson Laboratory) to generate mice deficient for CLEC-2 on platelets (*Clec-2*$^{f/f}$*;Pf4Cre* mice).

Clec-2$^{-/-}$[9], *Rag1*$^{-/-}$ (Jackson Laboratories)[32], and S1Pless mice[13] were previously described. Mice were housed in specific pathogen–free barrier facilities. All mice were of mixed genetic background (129S and C57BL/6J) unless otherwise stated. Sex- and age-matched WT littermate controls were used for all experiments. Mice were included in studies if they exhibited more than 75% for PDPN deficiency and 95% for CLEC-2 deficiency. Random assignment to treatment groups was used in antibody blocking and platelet transfusion studies in vivo. No blinding was used in this study. Animal studies were approved by the Institutional Animal Care and Use Committee of the Oklahoma Medical Research Foundation.

Microscopy

Organs were photographed at autopsy. For histology, samples were fixed in 4% paraformaldehyde (PFA) overnight at 4°C, washed, and embedded in paraffin. Sections (5 μm) were stained with H&E. Confocal microscopy was performed as previously described[8]. Briefly, tissues were fixed in 4% PFA overnight at 4°C, washed in PBS, cryoprotected in 20% sucrose in PBS at 4°C overnight, embedded in 50% Tissue Freezing Medium/50% OCT, and cryosectioned (20–30 μm). Sections were blocked for 1 hr at room temperature and incubated with primary antibodies overnight at 4°C. Secondary antibodies were added for 1 hr at room temperature. Primary antibodies were to murine thrombocytes (Accurate Chemical & Scientific Corp.), PDPN (clone 8.1.1, Developmental Studies Hybridoma Bank), CD41 (clone MWReg30, eBioscience), PDGFRβ (Santa Cruz), CD31 (clone 2H8, Abcam), CD31 (clone MEC13.3, BD Pharmingen), Ter119 (BD Pharmingen), PNAd (clone MECA-79, Biolegend), ER-TR7 (BioLegend), VE-cadherin (clone 11D4.1, BD Pharmingen), N-cadherin (Abcam), β-catenin (clone 14, BD Pharmingen), MAdCAM-1 (clone MECA-367, from Dr. Eugene Butcher, Department of Pathology, Stanford University School of Medicine, California, USA), as well as biotinylated-goat anti-mouse Lyve-1

(R&D Systems). Corresponding secondary antibodies were labelled with DyLight 488, AlexaFlour 555, or DyLight 649 (Jackson ImmunoResearch). Alternatively, Cy3-conjugated anti-αSMA (clone 1A4, Sigma Aldrich) was also used. Images were collected using an Olympus IX81 with DSU spinning-disk confocal microscope and a Hamamatsu ORCA-R^2 camera. Images were analysed using Slidebook 5.0 (Intelligent Imaging Innovations).

Immunoblotting

As previously described[8], tissues were collected, homogenized, and total protein concentration was calculated using a spectrophotometer (Eppendorf). Tissue lysates containing 20 μg total protein were resolved on a 10% SDS-PAGE resolving gel and transferred to an Immobilon-P membrane (EMD Millipore). Membranes were probed with a Syrian hamster anti-mouse PDPN (clone 8.1.1), rat anti-mouse VE-cad (clone BV13, Abcam), or mouse anti-GAPDH mAbs. Membranes were washed and probed with horseradish peroxidase-conjugated secondary antibodies. Signal was developed using ECL reagents (Thermo Scientific).

Bone marrow chimaeras

Bone marrow cells from both femurs and tibias were collected from WT and a limited number of *Clec-2*$^{-/-}$ mice that survived after weaning in our facility by flushing the marrow cavity with 5 ml of HBSS containing 1 mM EDTA, as previously described[8]. The cell suspension was then run through a 100 μm mesh cell strainer to remove aggregates, centrifuged at 300 x g for 8 min, and resuspended in sterile saline. Cells (5×10^6) in 200 μl saline were injected retro-orbitally into WT recipient mice that had been irradiated with 1100 rad. Engraftment efficiency was determined using flow cytometry analysis on a FACSCalibur (Becton Dickinson) with an antibody against CLEC-2 (clone 17D9, from Dr. Caetano Sousa, Immunobiology Laboratory, Cancer Research U.K., London Research Institute, London, U.K.)[36].

Flow cytometric analysis of PDPN expression in LNs

PDPN expression on LN cells was analysed by flow cytometry. Briefly, LNs were digested in digestion buffer (RPMI-1640 (Invitrogen) containing 0.2 mg/ml collagenase P (Roche), 0.1 mg/ml DNase I (Invitrogen), and 0.8 mg/ml Dispase (Roche)) at 37°C for 20 min. Digested LNs were vigorously mixed to ensure disruption of capsule and release of leukocytes. Cell suspensions were placed in ice-cold PBS containing 2% FCS and 5 mM EDTA and centrifuged at 300 x g for 10 min at 4°C. Pellets were resuspended in digestion buffer. Washed cells (5×10^6) were blocked for 15 min on ice (in HBSS containing Ca^{2+} and Mg^{2+}, 2 % horse serum, 20 μg/ml anti-CD16/CD32 (2.4G2, BD Pharmingen)). Isolated cells were incubated with antibodies to PDPN (clone 8.1.1) and biotinylated CD31 (clone MEC13.3, BD Pharmingen) for 30 min on ice and washed. Cells were then incubated with fluorescent dye-conjugated antibodies: AF488-conjugated goat anti-Syrian hamster IgG (Jackson ImmunoResearch), PerCP-conjugated streptavidin (BioLegend), and PE-conjugated rat anti-mouse CD45 (clone 30-F11, BD Pharmingen) for 20 min on ice. Flow cytometry analysis was performed on a FACSCalibur (Becton Dickinson).

Postnatal CLEC-2 depletion

WT and *Rag1*$^{-/-}$ mice were intraperitoneally (i.p.) injected with 8 μg/g body weight of a mAb to CLEC-2 (clone INU1)[19] at P1, 6, and 11. These mice were then sacrificed on P15.

Labelling of erythrocytes or platelets

For erythrocyte labelling, whole blood from WT mice was collected into EDTA-coated Microvette 500 K3E tubes (Sarstedt), washed in HBSS (without Ca^{2+} and Mg^{2+}), and centrifuged at 1200 x g for 10 min. Cells were resuspended in HBSS (without Ca^{2+} and Mg^{2+}) at a 1:5 dilution of the original volume and incubated with 5 μM CM-DiI (Invitrogen). Washed, labelled RBCs were resuspended at a 75% hematocrit, and 200 μl were intravenously injected into mice. For platelet labelling, platelet-rich plasma was obtained by collecting whole blood into an Eppendorf tube containing 20 IU heparin, adding 500 μl modified Tyrode's buffer (137 mM NaCl, 0.3 mM Na_2HPO_4, 2 mM KCl, 12 mM $NaHCO_3$, 5 mM HEPES, 5 mM glucose, pH 7.3) containing 0.35% BSA, and centrifuging for 8 min at 100 x g at room temperature. Platelets were collected by centrifuging for 10 min at 1000 x g. Washed platelets were incubated with 5 μM CellTracker Green (Invitrogen) for 30 min at 37°C. Labelled platelet-rich plasma was washed in HBSS (without Ca^{2+} and Mg^{2+}) and resuspended in HBSS (without Ca^{2+} and Mg^{2+}) prior to intravenous injection. Efficiency of labelling was confirmed using a FACSCalibur (Becton Dickinson) and analyzed using CellQuest Pro (Becton Dickinson).

Vascular permeability analysis

To determine the vascular permeability in MLNs, 250 μg of lysine-fixable FITC-dextran (2,000 kDa, Invitrogen) in 40 μl total volume physiologic saline was injected into the superior mesenteric artery that feeds MLNs immediately before sacrificing animals. Frozen sections of MLNs were stained with anti-CD31 or PNAd antibodies and analysed for the presence of dextran outside the blood vessels. Alternatively, 500 μg of lysine-fixable FITC-dextran (2,000 kDa, Invitrogen) or fluorescently labelled RBCs resuspended at a 75% hematocrit were intravenously injected into mice 1 min or 10 min, respectively, prior to sacrificing mice. Frozen sections of LN were stained with an anti-CD31 antibody and analysed for the presence of fluorescently labelled RBCs outside the blood vessels. Evans blue dye (2% in saline) was intravenously injected 5 min prior to sacrificing the mice. Mice were perfused with heparanized saline and LNs were placed in formamide (Fisher Scientific) overnight at 55°C. Tissues were removed from formamide, and absorbance was measured at 620 nm in a spectrophotometer[33].

Transmission electron microscopy (TEM)

LNs were removed and fixed overnight at 4°C in 2% gluteraldehyde in 0.1 M cacodylate buffer (pH 7.3). Tissues were washed in 0.1 M cacodylate buffer and post-fixed in 1% osmium tetroxide (1.5 hrs) and 1% tannic acid (1 hr). Tissues were dehydrated through graded alcohols and embedded in Epon resin (EMS). Semi-thin sections (~300 nm) were cut using an ultramicrotome (RMC 7000, RMC) equipped with a diamond knife and stained with toluidine blue, some of which were imaged. Ultrathin sections (~70 nm) were stained with uranyl acetate and lead citrate and visualised using a Hitachi H-7600 electron

microscope with a 4 megapixel digital monochrome camera and AMT-EM image acquisition software (Advanced Microscopy Techniques).

Platelet transfusion experiments

Platelets were isolated as described above and were intravenously injected into *Clec-2*$^{-/-}$ BM chimaeras once a day for 4 consecutive days. For S1Pless mice, WT or *Clec-2*$^{-/-}$ platelets were isolated as before and resuspended in HBSS without Ca^{2+} and Mg^{2+}. Either WT or *Clec-2*$^{-/-}$ platelets were administered once a day for 4 consecutive days. One minute prior to sacrifice, mice were injected (i.v.) with 500 μg of FITC-Dextran (2,000 kDa, Invitrogen) in 100 μl HBSS without Ca^{2+} and Mg^{2+}.

Immune challenge

Three- to four-week-old mice received subcutaneous injections of 250 μg Ovalbumin/ Complete Freunds' Adjuvant (OVA/CFA) into the hindlimb[34]. Contralateral hindlimbs were injected with equivalent volume of saline as a control. Mice were sacrificed 1 week after challenge and popliteal LNs were processed for immunofluorescence staining.

L-selectin blockade of lymphocyte homing

Three- to four-week-old mice were challenged with 250 μg OVA/CFA into the hindlimb. Mice were then administered i.p. 30 μg of an anti-mouse L-selectin antibody (Mel-14)[20] every other day for one week. Mice were sacrificed and popliteal LNs were dissected and analysed.

In vitro leukocyte rolling assay

To determine the blocking efficiency of Mel-14, an in vitro lymphocyte rolling assay was used. Briefly, 100 μg/ml streptavidin was coated on 35-mm polystyrene dishes overnight at 4°C. After washing three times with HBSS, the dishes were blocked with 1% human serum albumin in HBSS for 2 hr at 4°C and then incubated with biotin conjugated 6-sulfo-sLe^{x}, a ligand for L-selectin, for 2 hr at 4°C[35]. Isolation of peripheral leukocytes was described previously[36]. Briefly, heparinized blood was obtained from WT or *Pdpn*$^{f/f}$*;CagCre* mice that were treated with Mel-14 or rat IgG. After lysis of red blood cells, leukocytes were centrifuged at 100 x g for 10 min. Leukocytes (0.1×10^6/ml) were perfused over 6-sulfo-sLe^{x} coated surface under shear stress at 1.0 dyn/cm^2. The number of rolling cells was counted using the Element software (Nikon).

In vivo blockade of VE-cad and integrin αIIbβIIIa

After hindlimb challenge with OVA/CFA, mice were i.p. injected with 30 μg every other day of a mAb against VE-cad (clone 11D4.1, BD Pharmingen) or against GPIIbIIIa (clone JON/A)[37]. One week after immune challenge, Evans blue dye permeability assays were performed as described above.

Peripheral lymphocyte counts

For measuring peripheral lymphocyte counts, whole blood obtained in EDTA-coated tubes was used to obtain a complete blood count using a Hemavet.

Development of PDPN$^+$ and PDPN$^-$ cell line

Parental murine melanoma cell line B16-F0, which contains PDPN$^+$ and PDPN$^-$ cells, was purchased from American Type Culture Collection (ATCC). Cells were cultured in Dulbecco's modified Eagle's medium (DMEM) containing 10% heat-inactivated fetal bovine serum (FBS) and 1% L-glutamine/penicillin/streptomycin (Cellgro) at 37°C in a humidified atmosphere of 5% CO_2. B16-F0 cells were stained with anti-murine PDPN mAb (clone 8.1.1) and a DyLight488-conjugated secondary antibody. Stained cells were then sorted with a FACSAria III cell sorter (BD Biosciences) to generate the PDPN$^+$ and PDPN$^-$ B16-F0 cells.

Analysis of S1P concentration

Platelets were isolated from WT or CLEC-2 deficient mice as before. After being washed with modified Tyrode's buffer containing 0.35% fatty acid-free BSA, platelets (1×10^8 in 100 μl) were then incubated with a mAb against CLEC-2 (clone INU1 at 10 μg/ml) for 10 min. at room temperature. S1P concentration was determined using an S1P ELISA kit (Echelon Biosciences) according to manufacturer's protocol. Alternatively, platelets were incubated with 5×10^5 PDPN$^+$ or PDPN$^-$ cells for 10 min. at room temperature. Then, the supernatant was collected and S1P concentration was quantitated by electrospray ionisation tandem mass spectrometry (ESI-MS/MS) using stable isotope dilution with heptadeuterated S1P (Avanti Polar Lipids) as the internal standard as described previously[38].

Ex vivo LN slice culture

MLNs were dissected from WT and PDPN-deficient mice and embedded in low melting point agarose (Invitrogen) at 37°C. Blocks were cooled on ice and sectioned (~250 mm) using a Vibratome (McIlwain tissue chopper). LN slices were then coincubated with washed platelets (2×10^7 in 100 μl of RPMI 1640 containing 10% charcoal stripped FBS; Invitrogen) and isolated from WT, *Clec-2*$^{-/-}$, or S1Pless mice, for 1.5 hrs at 37°C while shaking gently. In some experiments, normal FBS or the S1PR1 antagonist, W146 (5 μM, Cayman Chemical), was included. MLN slices were then fixed in 4% PFA in PBS for 30 min and processed for cryopreservation. Cryosections were stained with antibodies against CD31 (clone 2H8, Abcam) and VE-cad (clone 11D4.1, BD Pharmingen).

Quantification of PDPN deletion, dextran leakage, or VE-cad intensity

PDPN levels were calculated using ImageJ software to compare the mean intensities between the groups from a minimum of 5 low magnification (10x) images. For quantification of FITC-dextran leakage, six cryosections were cut per mouse and each section was analysed for the total number of HEVs (~50/section of MLNs) and non-HEVs based on CD31 or PNAd staining and morphology. The number of vessels that exhibited dextran outside the vessel was determined and the percentage of "leaky" vessels compared to the total number of that vessel type was determined. Similarly, the percentage of VE-cad expression on vessels from MLN cryosections was determined by comparing the number HEV and non-HEV that were VE-cad positive to the total number of vessel type. Alternatively, VE-cad intensities on HEVs were determined using image J analysis software.

Statistical analysis

Statistical tests were performed using Prism software (GraphPad). Two-sided, Student t-tests were performed after the data were confirmed to fulfill the criteria of normal distribution and equal variance. Differences were considered statistically significant when $P < 0.05$.

Supplementary Material

Refer to Web version on PubMed Central for supplementary material.

Acknowledgments

We thank Paul Kincade and Linda Thompson for critical reading of the manuscript, Ralf Adams for providing *PdgfrbCre* mice, and Michael Kinter and Caleb Marlin for technical assistance. Work was supported by grants from the National Institute of Health (GM103441, GM097747, HL085607, HL093242, HL103432, HL65590, HL112788), VA Merit Award (BX001984), The Deutsche Forschungsgemeinschaft (SFB688), Chinese National Natural Science Foundation (30928010), Jiangsu Provincial Special Program of Medical Science (BL2012005), Jiangsu Province's Key Medical Center (ZX201102), and American Heart Association (SDG7410022).

References

1. Butcher EC, Picker LJ. Lymphocyte homing and homeostasis. Science. 1996; 272:60–66. [PubMed: 8600538]
2. Drayton DL, Liao S, Mounzer RH, Ruddle NH. Lymphoid organ development: from ontogeny to neogenesis. Nature Immunol. 2006; 7:344–353. [PubMed: 16550197]
3. Girard JP, Moussion C, Forster R. HEVs, lymphatics and homeostatic immune cell trafficking in lymph nodes. Nature Rev Immunol. 2012; 12:762–773. [PubMed: 23018291]
4. Rosen SD. Ligands for L-selectin: homing, inflammation, and beyond. Annu Rev Immunol. 2004; 22:129–156. [PubMed: 15032576]
5. von Andrian UH, Mempel TR. Homing and cellular traffic in lymph nodes. Nature Rev Immunol. 2003; 3:867–878. [PubMed: 14668803]
6. Breiteneder-Geleff S, et al. Podoplanin, novel 43-kd membrane protein of glomerular epithelial cells, is down-regulated in puromycin nephrosis. Am J Pathol. 1997; 151:1141–1152. [PubMed: 9327748]
7. Farr AG, et al. Characterization and cloning of a novel glycoprotein expressed by stromal cells in T-dependent areas of peripheral lymphoid tissues. J Exp Med. 1992; 176:1477–1482. [PubMed: 1402691]
8. Fu J, et al. Endothelial cell O-glycan deficiency causes blood/lymphatic misconnections and consequent fatty liver disease in mice. J Clin Invest. 2008; 118:3725–3737. [PubMed: 18924607]
9. Bertozzi CC, et al. Platelets regulate lymphatic vascular development through CLEC-2-SLP-76 signaling. Blood. 2010; 116:661–670. [PubMed: 20363774]
10. Watson SP, Herbert JM, Pollitt AY. GPVI and CLEC-2 in hemostasis and vascular integrity. J Thromb Haemost. 2010; 8:1456–1467. [PubMed: 20345705]
11. Carmeliet P, et al. Targeted deficiency or cytosolic truncation of the VE-cadherin gene in mice impairs VEGF-mediated endothelial survival and angiogenesis. Cell. 1999; 98:147–157. [PubMed: 10428027]
12. Grazia Lampugnani M, et al. Contact inhibition of VEGF-induced proliferation requires vascular endothelial cadherin, beta-catenin, and the phosphatase DEP-1/CD148. J Cell Biol. 2003; 161:793–804. [PubMed: 12771128]
13. Camerer E, et al. Sphingosine-1-phosphate in the plasma compartment regulates basal and inflammation-induced vascular leak in mice. J Clin Invest. 2009; 119:1871–1879. [PubMed: 19603543]

14. Gaengel K, et al. The sphingosine-1-phosphate receptor S1PR1 restricts sprouting angiogenesis by regulating the interplay between VE-cadherin and VEGFR2. Dev Cell. 2012; 23:587–599. [PubMed: 22975327]
15. Soderberg KA, et al. Innate control of adaptive immunity via remodeling of lymph node feed arteriole. Proc Natl Acad Sci USA. 2005; 102:16315–16320. [PubMed: 16260739]
16. Goerge T, et al. Inflammation induces hemorrhage in thrombocytopenia. Blood. 2008; 111:4958–4964. [PubMed: 18256319]
17. Renz H, Brandtzaeg P, Hornef M. The impact of perinatal immune development on mucosal homeostasis and chronic inflammation. Nature Rev Immunol. 2012; 12:9–23. [PubMed: 22158411]
18. Chyou S, et al. Fibroblast-type reticular stromal cells regulate the lymph node vasculature. J Immunol. 2008; 181:3887–3896. [PubMed: 18768843]
19. May F, et al. CLEC-2 is an essential platelet-activating receptor in hemostasis and thrombosis. Blood. 2009; 114:3464–3472. [PubMed: 19641185]
20. Gallatin WM, Weissman IL, Butcher EC. A cell-surface molecule involved in organ-specific homing of lymphocytes. Nature. 1983; 304:30–34. [PubMed: 6866086]
21. Diacovo TG, et al. Platelet-mediated lymphocyte delivery to high endothelial venules. Science. 1996; 273:252–255. [PubMed: 8662511]
22. Dejana E, Tournier-Lasserve E, Weinstein BM. The control of vascular integrity by endothelial cell junctions: molecular basis and pathological implications. Dev Cell. 2009; 16:209–221. [PubMed: 19217423]
23. Hodivala-Dilke KM, et al. Beta3-integrin-deficient mice are a model for Glanzmann thrombasthenia showing placental defects and reduced survival. J Clin Invest. 1999; 103:229–238. [PubMed: 9916135]
24. Ulrych T, et al. Release of sphingosine-1-phosphate from human platelets is dependent on thromboxane formation. J Thromb Haemost. 2011; 9:790–798. [PubMed: 21251196]
25. Pappu R, et al. Promotion of lymphocyte egress into blood and lymph by distinct sources of sphingosine-1-phosphate. Science. 2007; 316:295–298. [PubMed: 17363629]
26. Gretz JE, Anderson AO, Shaw S. Cords, channels, corridors and conduits: critical architectural elements facilitating cell interactions in the lymph node cortex. Immunol Rev. 1997; 156:11–24. [PubMed: 9176696]
27. Katakai T, et al. Lymph node fibroblastic reticular cells construct the stromal reticulum via contact with lymphocytes. J Exp Med. 2004; 200:783–795. [PubMed: 15381731]
28. Boulaftali Y, et al. Platelet ITAM signaling is critical for vascular integrity in inflammation. J Clin Invest. 2013; 123:908–916. [PubMed: 23348738]
29. Hayashi S, McMahon AP. Efficient recombination in diverse tissues by a tamoxifen-inducible form of Cre: a tool for temporally regulated gene activation/inactivation in the mouse. Dev Biol. 2002; 244:305–318. [PubMed: 11944939]
30. Foo SS, et al. Ephrin-B2 controls cell motility and adhesion during blood-vessel-wall assembly. Cell. 2006; 124:161–173. [PubMed: 16413489]
31. Kisanuki YY, et al. Tie2-Cre transgenic mice: a new model for endothelial cell-lineage analysis in vivo. Dev Biol. 2001; 230:230–242. [PubMed: 11161575]
32. Mombaerts P, et al. RAG-1-deficient mice have no mature B and T lymphocytes. Cell. 1992; 68:869–877. [PubMed: 1547488]
33. Han ED, et al. Increased vascular permeability in C1 inhibitor-deficient mice mediated by the bradykinin type 2 receptor. J Clin Invest. 2002; 109:1057–1063. [PubMed: 11956243]
34. Kamala T. Hock immunization: a humane alternative to mouse footpad injections. J Immunol Methods. 2007; 328:204–214. [PubMed: 17804011]
35. Lou J, et al. Flow-enhanced adhesion regulated by a selectin interdomain hinge. J Cell Biol. 2006; 174:1107–1117. [PubMed: 17000883]
36. Xia L, et al. P-selectin glycoprotein ligand-1-deficient mice have impaired leukocyte tethering to E-selectin under flow. J Clin Invest. 2002; 109:939–950. [PubMed: 11927621]

37. Bergmeier W, et al. Flow cytometric detection of activated mouse integrin alphaIIbbeta3 with a novel monoclonal antibody. Cytometry. 2002; 48:80–86. [PubMed: 12116368]

38. Selim S, et al. Plasma levels of sphingosine 1-phosphate are strongly correlated with haematocrit, but variably restored by red blood cell transfusions. Clin Sci. 2011; 121:565–572. [PubMed: 21749329]

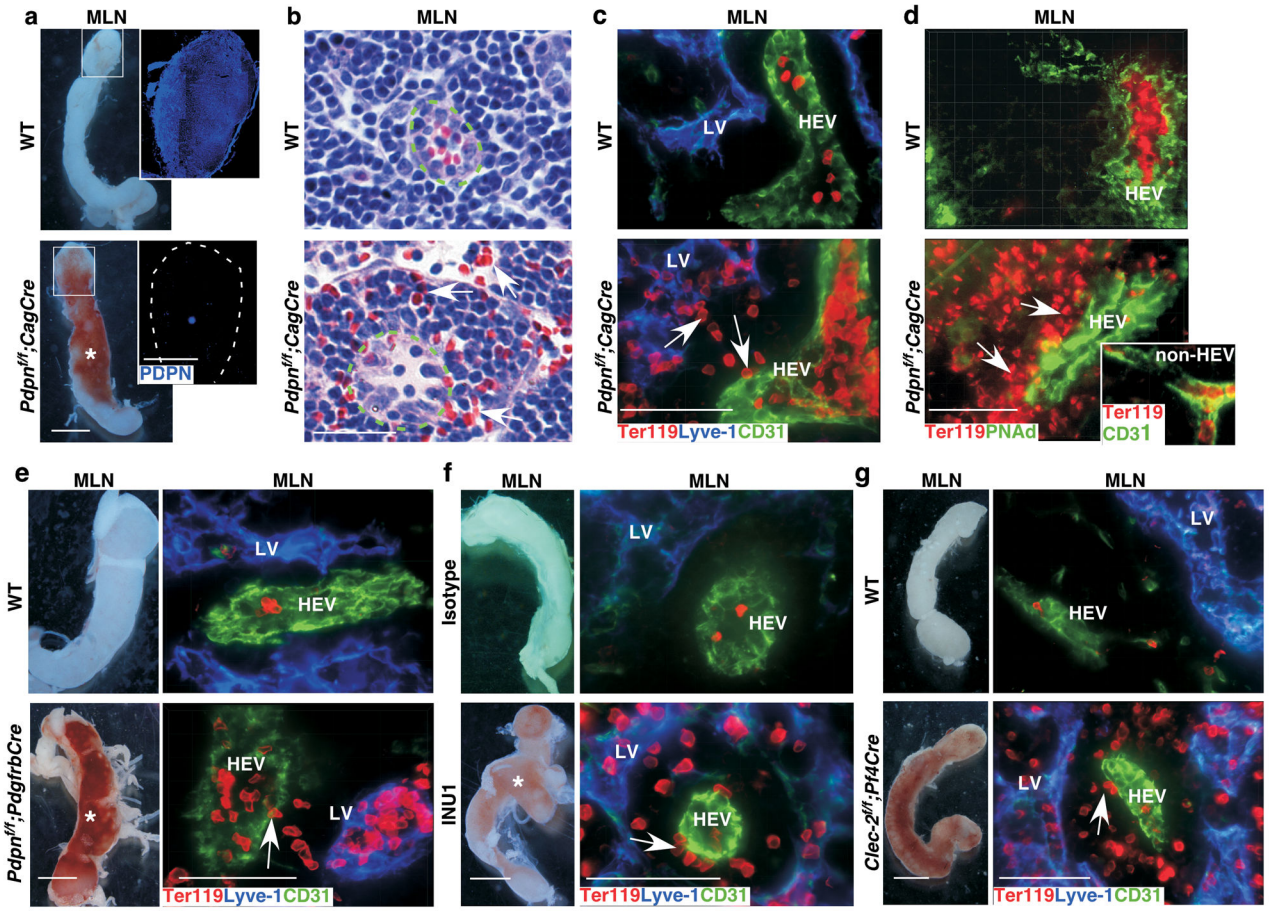

Figure 1. Loss of FRC PDPN or platelet CLEC-2 leads to spontaneous mucosal LN bleeding

a, Gross morphology of MLNs. Insets contain montages of confocal images of MLN cryosections showing PDPN expression in WT and *Pdpn*$^{f/f}$*;CagCre* mice. **b**, Images of H&E–stained MLN sections. Arrows indicate extravasated RBCs outside HEVs (dashed line) of *Pdpn*$^{f/f}$*;CagCre* mice. **c,** Confocal images of MLNs from WT and *Pdpn*$^{f/f}$*;CagCre* mice reveal extravasated RBCs (arrows) outside HEVs, some of which are picked up by lymphatic vessels (LVs). Ter119 indicates RBCs. CD31 marks endothelial cells. Lyve-1 marks LVs. **d**, Immunostaining of MLN cryosections using HEV-specific marker PNAd. Inset shows that no bleeding occurred around CD31^{+}/PNAd^{-} non-HEV vessels in MLNs. **e,** Gross morphology and confocal images of MLN cryosections from WT and *Pdpn*$^{f/f}$*;PdgfrbCre* stained for Ter119, Lyve-1, and CD31. **f,** Gross morphology and confocal images of MLNs from P15 WT mice treated with isotype control rat IgG1κ or the CLEC-2 depleting antibody, INU1. **g,** Gross morphology and confocal images of MLN cryosections from WT and *Clec-2*$^{f/f}$*;Pf4Cre* mice stained for Ter119, Lyve-1, and CD31. Data are representatives of ≥ 12 mice/group. Scale bars, 2 mm (gross images), 50 μm (**b**, and confocal images). Asterisk indicates bleeding in the LN. Arrows indicate extravasated RBCs. Tissues were from 1-month-old mice unless otherwise specified.

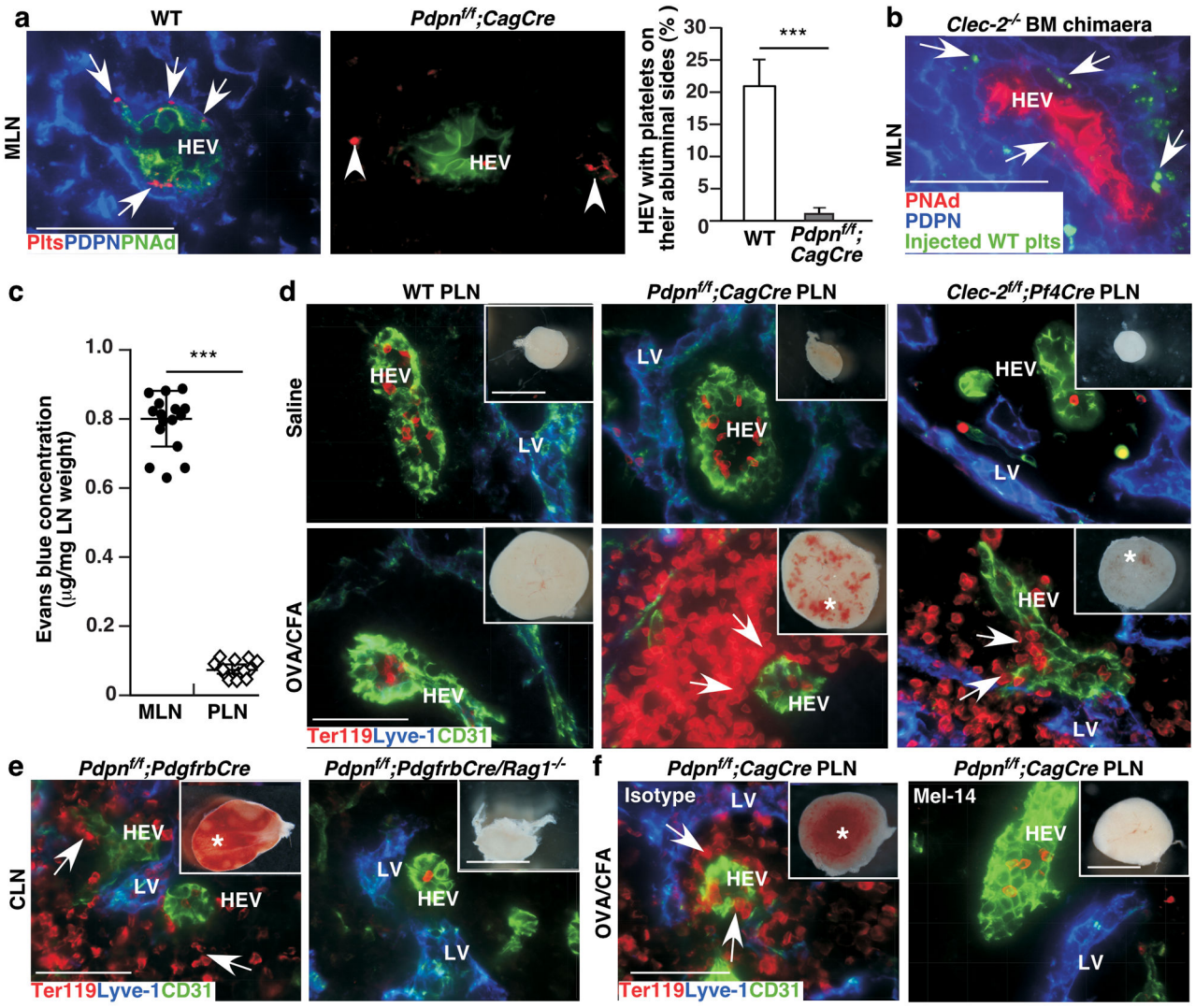

Figure 2. FRC PDPN and platelet CLEC-2 protect LN vascular integrity during immune responses

a, Confocal images of MLN cryosections stained with antibodies to PNAd, platelets, and PDPN. Arrows indicate platelets on the abluminal side of HEVs. Arrowheads indicate platelets that are not associated with HEVs. Bar graph on the right represents percentage of HEVs with platelets on their abluminal side (mean ± s.d., 250 HEVs/mouse (n = 3)). **b,** Confocal images of PNAd^{+}HEVs, PDPN, and transfused fluorescently labelled WT platelets (plts) in MLNs. Arrows indicate plts on the abluminal side of HEVs. **c,** Comparison of Evans blue permeability between MLNs and popliteal LNs (PLNs) of 1-month-old WT mice 5 min after intravenous injections (mean ± s.d., n = 15/group). **d,** Gross morphology (insets) and confocal images of PLNs after OVA/CFA challenge. **e,** Gross morphology (insets) and confocal images of CLNs from 3-week-old mice with (*Pdpn$^{f/f}$;PdgfrbCre*) or without (*Pdpn$^{f/f}$;PdgfrbCre/Rag1$^{-/-}$*) lymphocytes. **f,** Gross morphology (insets) and confocal images of PLNs from 1-month-old mice one week after OVA/CFA challenge and injections with a mAb (Mel-14) that blocks L-selectin-dependent lymphocyte homing or with an isotype control rat IgG. Data represent at least 8 LNs per group from at least three

experiments. Scale bars, 2 mm (gross), 50 μm (confocal). Asterisk indicates bleeding, and arrows mark extravasated RBCs around HEVs (**d-f**). ***, $P < 0.001$.

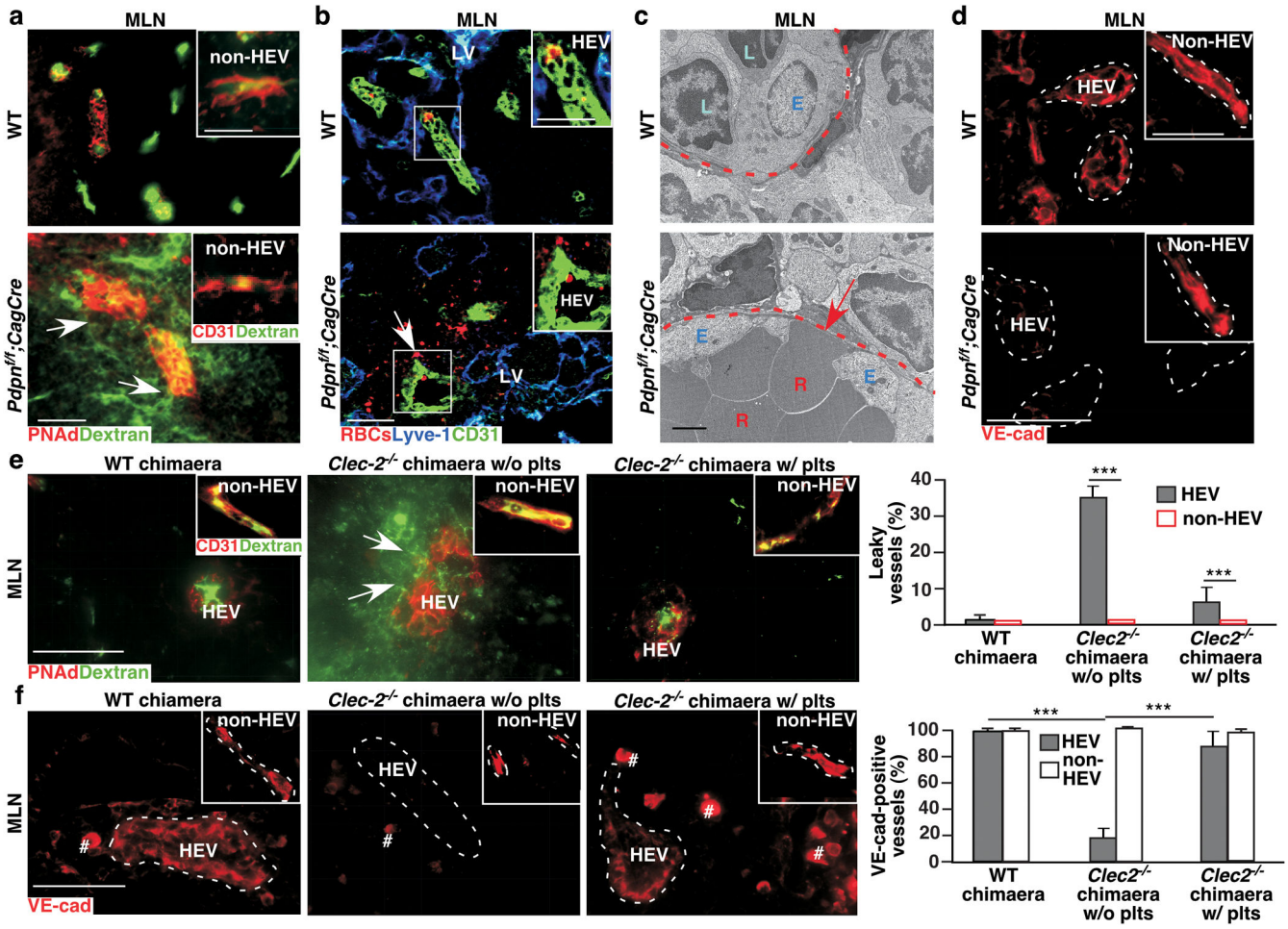

Figure 3. Interactions of FRC PDPN and platelet CLEC-2 are critical for HEV junctional integrity

a, Confocal images of intravenously injected FITC-dextran (2,000 kDa) in P15 MLNs. Arrows indicate vascular leak of FITC-dextran. Insets show non-HEVs blood vessels. **b,** Confocal images of intravenously injected/fluorescently labelled RBCs (red) in MLNs from 2-month-old mice. Arrow and insets show labelled RBCs outside of HEVs ($CD31^+$). **c,** Transmission electron micrographs of HEVs in MLNs. Arrow indicates gaps and RBCs between high endothelial cells. **d,** Confocal images of VE-cad in P8 MLNs. Insets show VE-cad staining in non-HEV blood vessels. **e,** Confocal analysis of intravenously injected FITC-dextran in MLNs from WT or *Clec2*$^{-/-}$ BM chimaeras with or without previous intravenous injections of WT platelets (plts). Arrows indicate vascular leak of FITC-dextran. Inset depicts non-HEV blood vessels. Graphs on the right quantify number of leaking vessels (mean ± s.d., 300 vessels per group (n = 3)). **f,** Immunofluorescence analysis of anti-VE-cad staining of HEVs and non-HEV blood vessels in WT BM chimaeras (WT chimaera), and *Clec2*$^{-/-}$ BM chimaeras (*Clec2*$^{-/-}$ chimaeras) without or with previous intravenous injections with WT plts. # indicates non-specific staining as also observed in negative controls. Graphs on the right quantify VE-cad staining (mean ± s.d., 300 vessels per group (n = 3)). Tissues were from 1-month-old (**a-c**) or 12-week post BM transplantation (**e, f**)

mice unless otherwise specified. Dashed lines mark HEVs. Data represent at least three individual experiments. Scale bars, 2 μm (TEM), 50 μm (confocal images (inset **a** and **b**, 25 μm)). ***, $P < 0.001$.

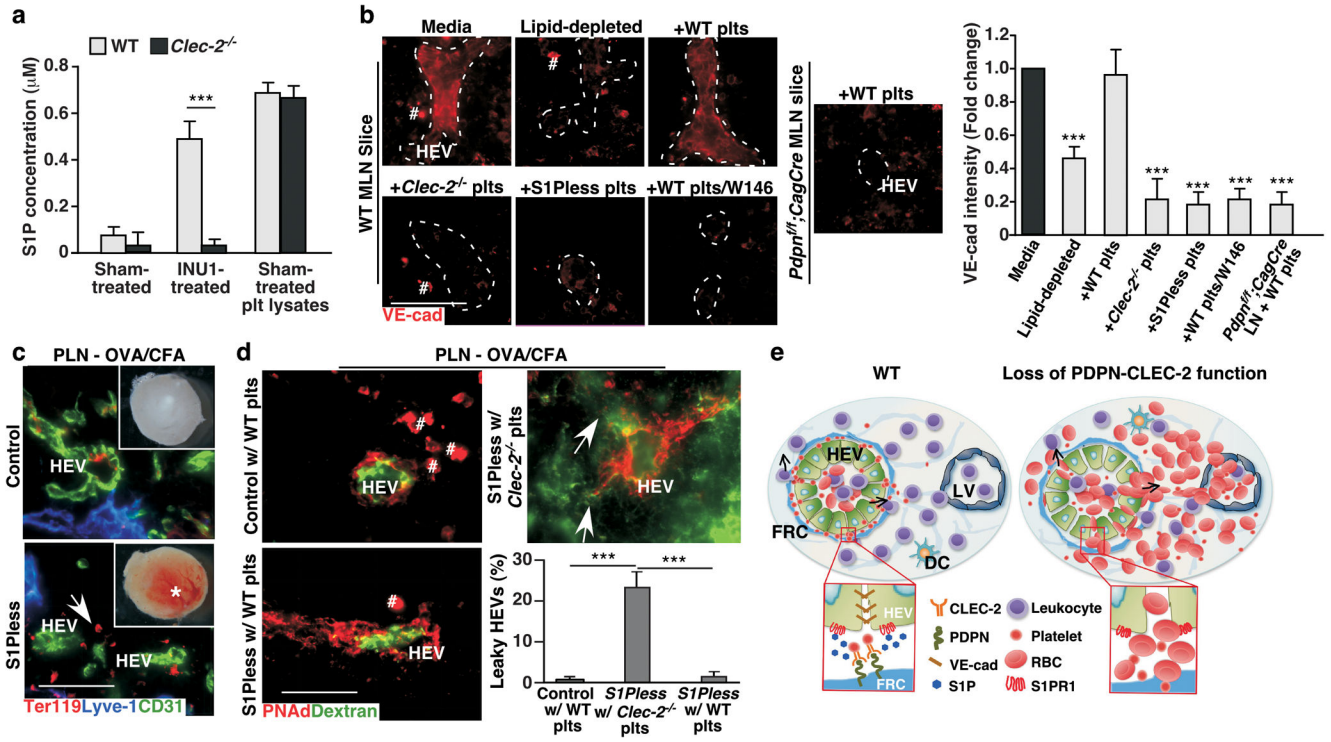

Figure 4. S1P from platelets after PDPN-CLEC-2-dependent activation contributes to HEV barrier function

a, ELISAs of S1P concentrations in supernatants of WT and *Clec-2*$^{-/-}$ platelets after incubation with CLEC-2 activating antibody, INU1 (INU1-treated) or isotype control rat IgG (sham-treated). S1P in platelet lysates (plt lysates) was used as the positive control (mean ± s.d., n = 4 mice per group representing two individual experiments). **b,** Representative images of VE-cad staining of HEVs from WT LN slices incubated for 1.5 hrs with DMEM and normal FBS (media), DMEM and lipid-depleted FBS (lipid-depleted), lipid-depleted and WT platelets (+WT plts), lipid-depleted and *Clec-2*$^{-/-}$ platelets (+*Clec-2*$^{-/-}$ plts), lipid-depleted and S1Pless platelets (+S1Pless plts), or lipid-depleted and WT plts plus S1PR1 antagonist W146 (+WT plts/W146). *Pdpn*$^{f/f}$*;CagCre* LN slices incubated with lipid-depleted and WT platelets (+WT plts) were controls. 100 HEVs analyzed per condition. Dashed lines mark HEVs. # marks non-specific staining as also observed in negative controls. Graphs represent ratios of VE-cad intensities on HEVs relative to that of WT LN slices cultured with media (mean ± s.d., n = 20 HEVs/group). **c,** Gross morphology (insets) and confocal images of draining popliteal LNs (PLN) after immunisation. Asterisk indicates bleeding. LV, lymphatic vessel (Lyve-1^{+}). Arrow marks bleeding (Ter119^{+}) around an HEV (CD31^{+}). **d**, Confocal images of PLN HEVs from S1Pless mice transfused with *Clec-2*$^{-/-}$ or WT platelets (plts) for 4 days and littermate controls transfused with WT plts after intravenous FITC-dextran injection. Arrows indicate vascular leak of FITC-dextran. Graphs on right quantify leaking HEVs (mean ± s.d., 50 HEVs/group (n = 3)). **e**, Model depicting how PDPN maintains HEV integrity during lymphocyte trafficking. FRC PDPN engages CLEC-2 on extravasated platelets in the perivenular space of HEVs and induces local release of S1P, which promotes VE-cad

expression on the WT HEV (left). In contrast, loss of the interaction results in impaired HEV integrity and subsequent bleeding (right). **b–d,** Data is from three individual experiments. Scale bars, 50 μm. ***, $P < 0.001$.